Supporting Information

Activating cobalt nanoparticles via the Mott-Schottky effect in nitrogen-rich carbon shells for base-free aerobic oxidation of alcohols to esters

Hui Su[1], Ke-Xin Zhang[1], Bing Zhang[1], Hong-Hui Wang[1], Qiu-Ying Yu[1], Xin-Hao Li[1], Markus Antonietti[2] and Jie-Sheng Chen[1]*

[1]School of Chemistry and Chemical Engineering, Shanghai Jiao Tong University, Shanghai 200240, P. R. China.

[2]Department of Colloid Chemistry, Max-Planck Institute of Colloids and Interfaces, Wissenschaftspark Golm, 14424 Potsdam, Germany.

*Corresponding authors. E-mail address: xinhaoli@sjtu.edu.cn (X. H. Li)

Experimental section

CO_2-TPD analysis: Temperature programmed desorption (TPD) was carried out by using CO_2 as the probe molecule. Sample was pre-treated in He flow at 150 ºC for 3h and cooled to room temperature. After being saturated with CO_2, the sample was purged with He for 1h at room temperature to sweep the physical molecule. Then sample was heated by 950 ºC at the rate of 15 ºC/min. The signals were monitored by a thermal conductivity detector (TCD).

EPR analysis: The tests were conducted with Bruker EMX-8/2.7C, with the following setting: center field: 3515 G, microwave frequency: 9.868 GHz, and power: 2.016 mW.

The nitrogen adsorption/desorption measurement: The tests were performed on a Micromeritics ASAP 2460 instrument.

XAFS measurement: The X-ray absorption data at the Co K-edge of the samples were recorded at room temperature in transmission mode using ion chambers at beamline BL14W1 of the Shanghai Synchrotron Radiation Facility (SSRF). The station was operated with a Si (111) double crystal monochromator. During the measurement, the synchrotron was operated at 3.5 GeV and the current was between 150-210 mA. The data for each sample were collected three times and calibrated with standard Ti and Co metal foil. Data processing was performed using the program ATHENA.

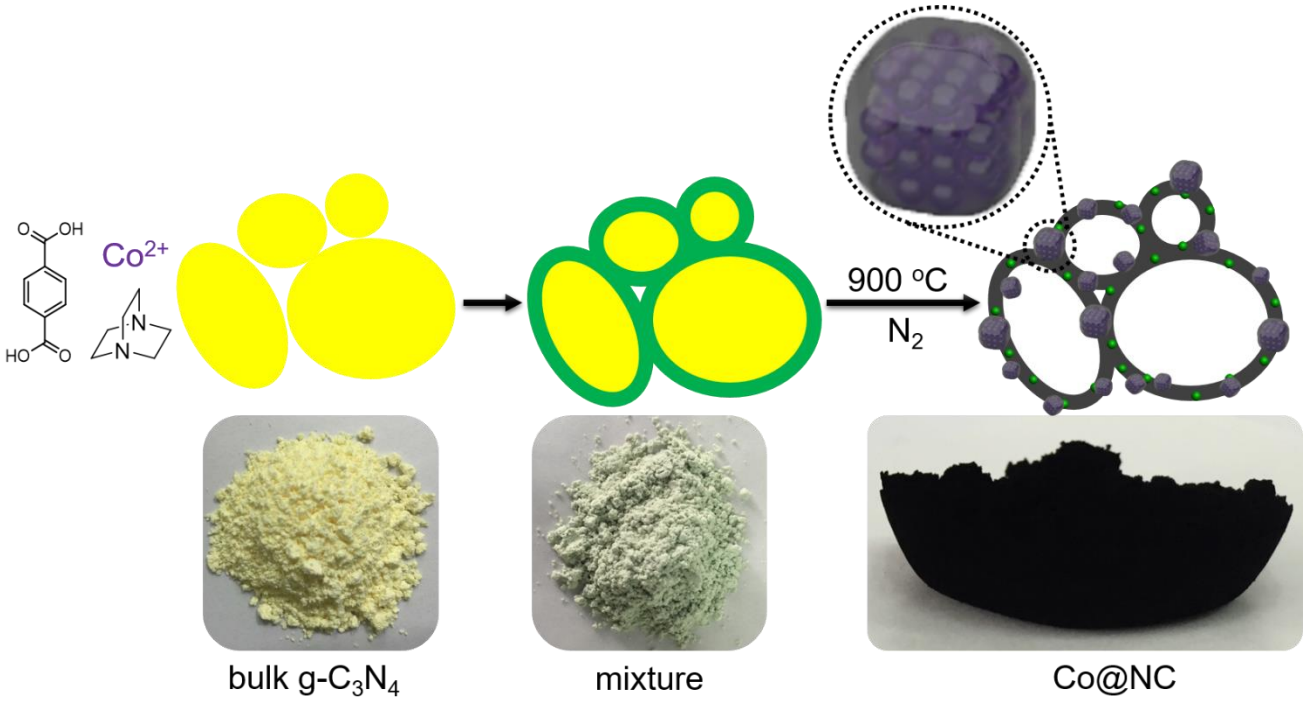

Figure S1. Synthetic process for Co@NC-x samples.

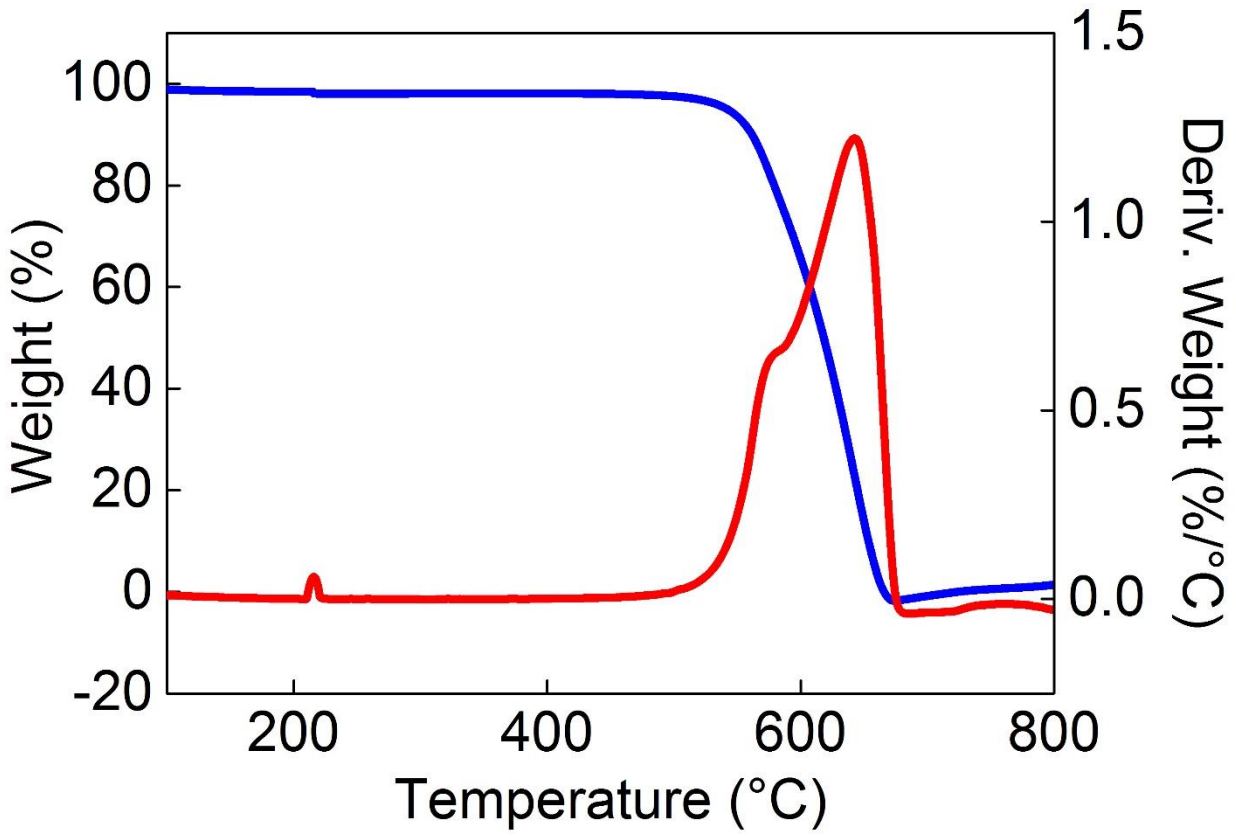

Figure S2. TGA-DTG analysis of g-C_3N_4 powder used for the synthesis of Co@NC-x. The g-C_3N_4 sample was heated under the flow of N_2 to 800 °C with a heating rate of 10 °C min^{-1}. The rapid weight loss happened from 520 °C. The complete decomposition of g-C_3N_4 could be achieved at a temperature around 680 °C.

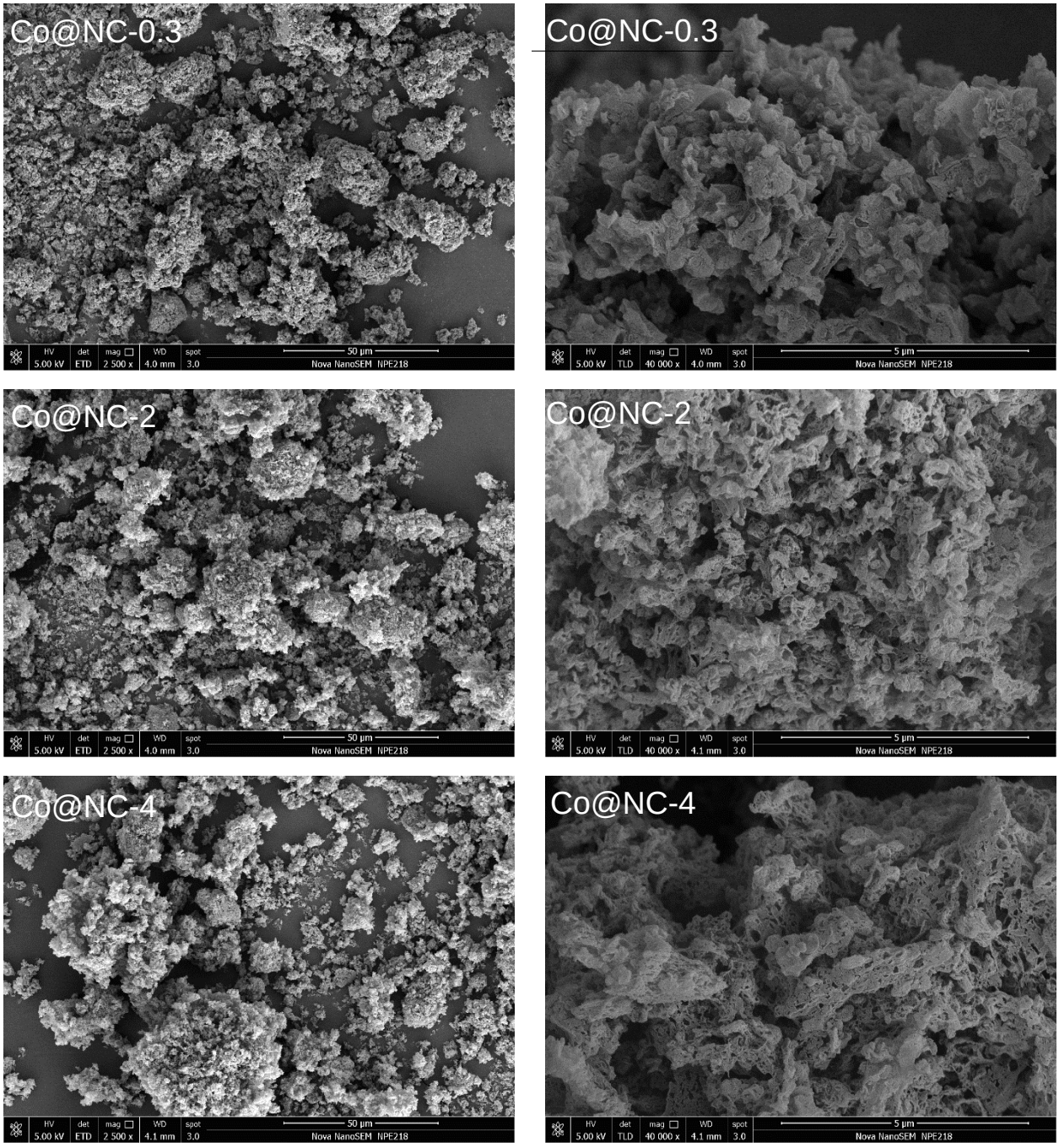

Figure S3. Typical SEM images of different Co@NC-x samples. All samples are carbon foam.

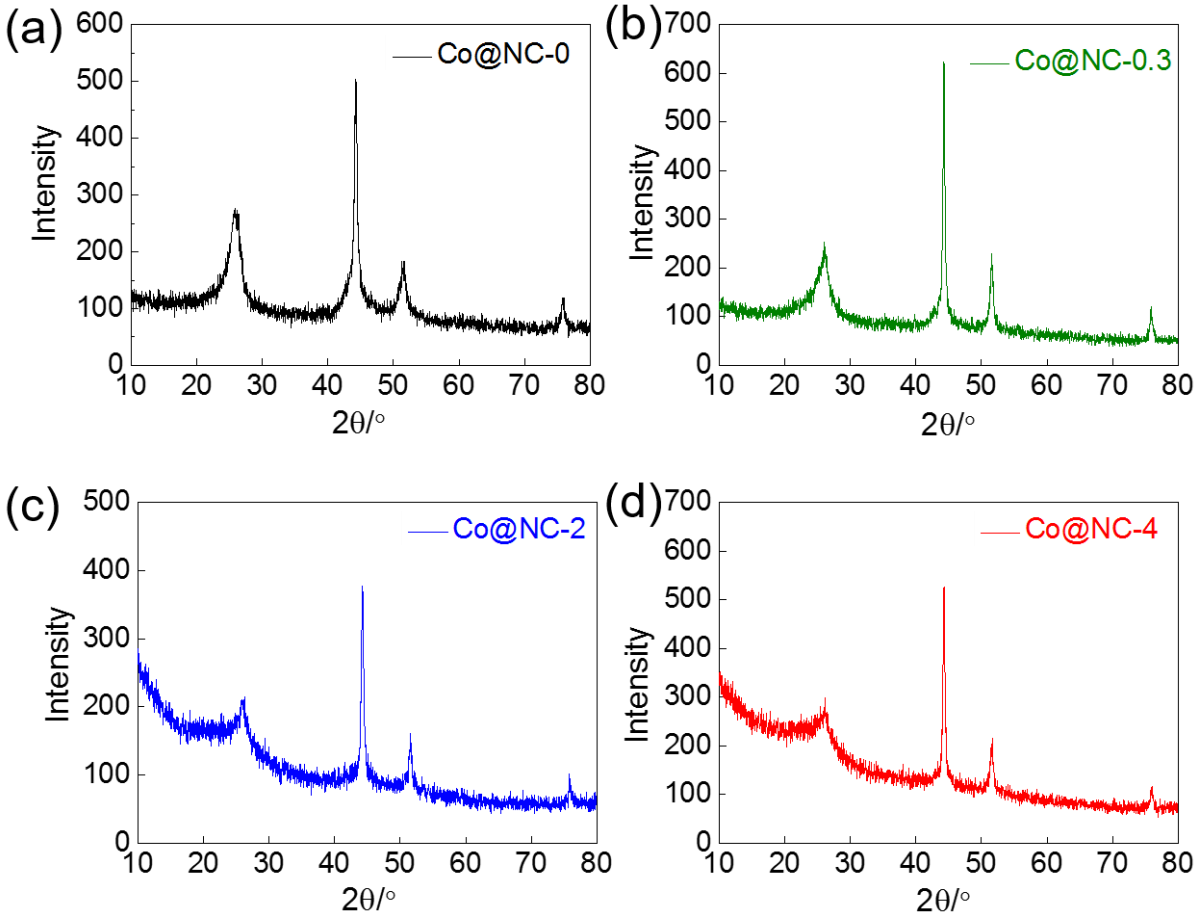

Figure S4. XRD patterns (a-d) of the Co@NC-x.

(a)

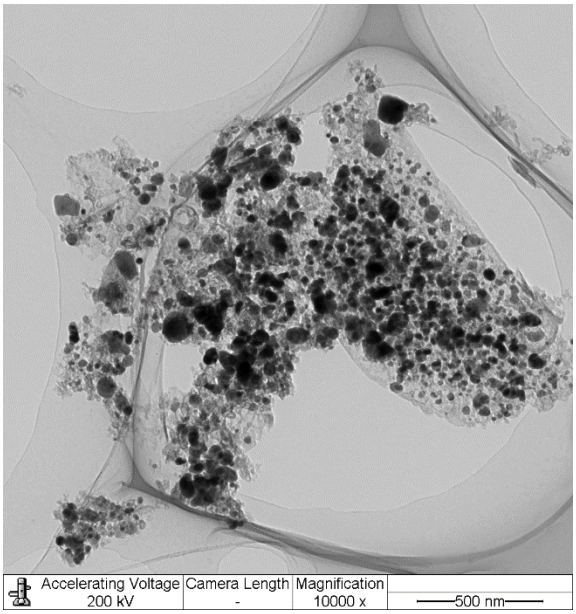

(b)

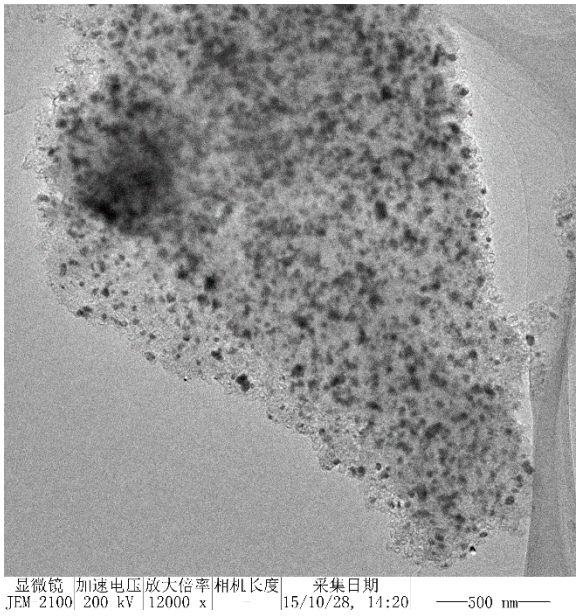

Figure S5. Typical TEM images of sample converted from homogeneous mixture of metal salt, 1,4-benzenedicarboxylic acid without triethylene diamine (a) and with triethylene diamine (b) molecules. It is observed that the absence of triethylene diamine organic ligand made Co nanoparticles further grow into large metal aggregations.

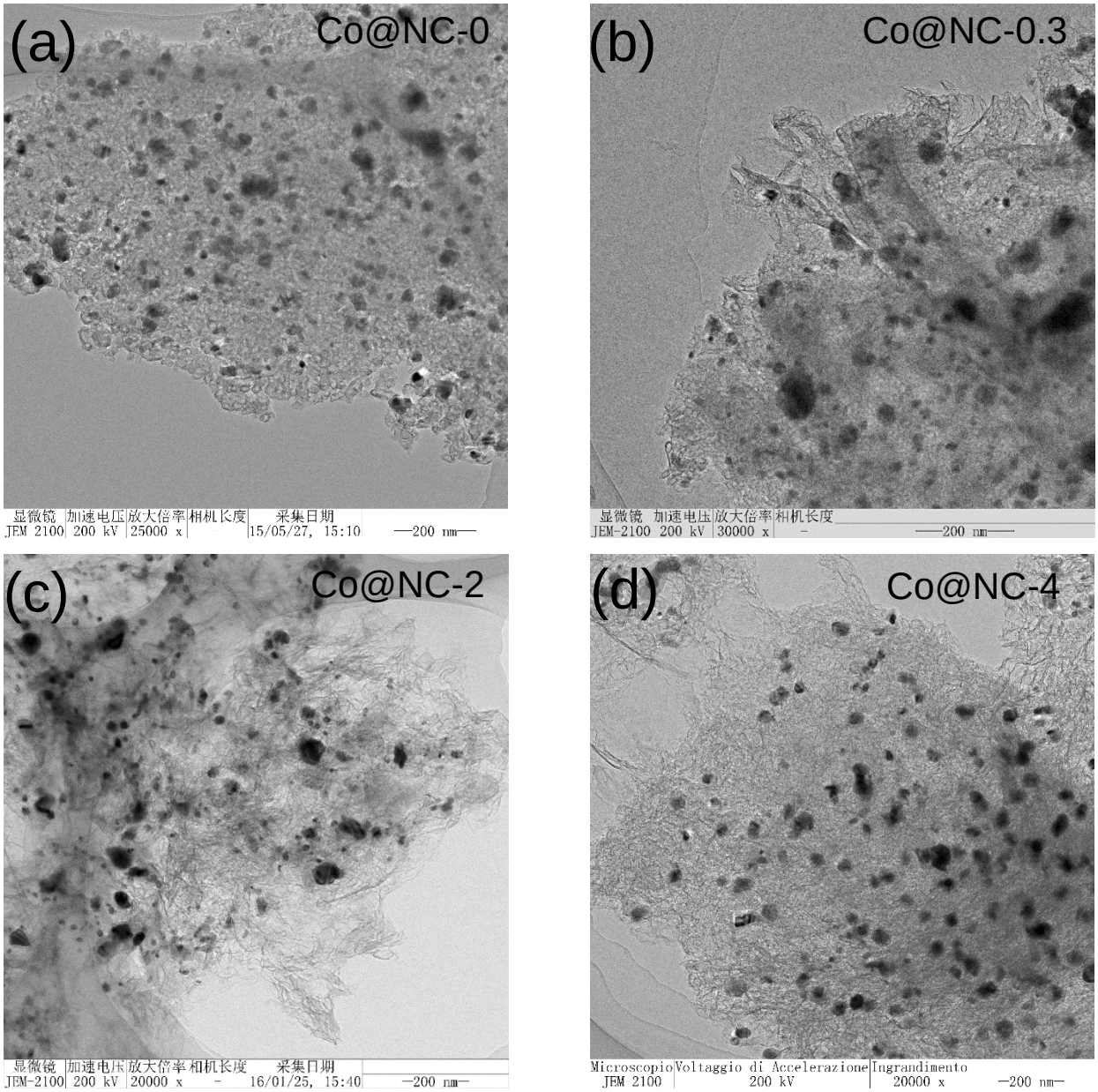

Figure S6. Typical TEM images of Co@NC-x samples. Increasing the amount of g-C_3N_4 in precursors made no obvious effect on metal particle size and nanostructure of Co nanoparticles and carbon support for Co@NC.

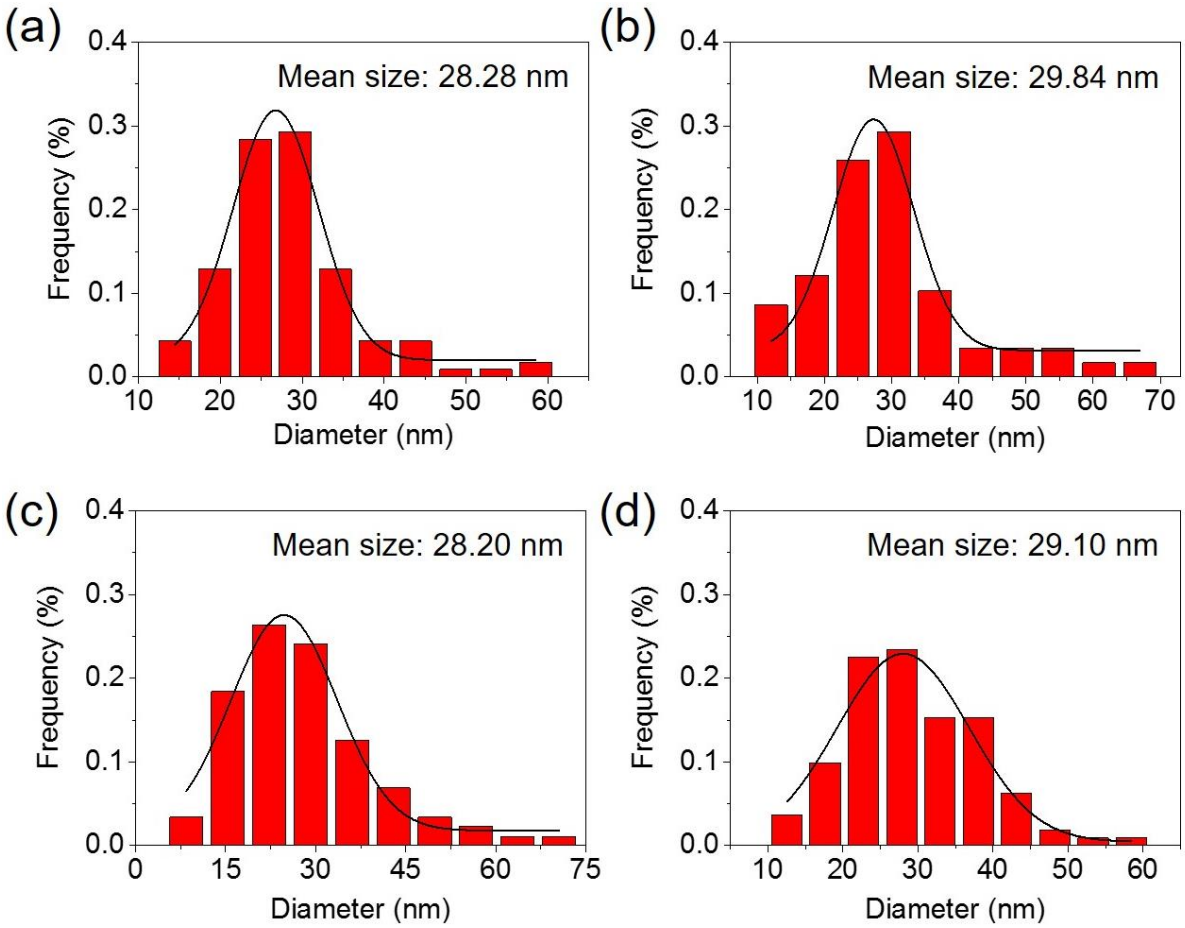

Figure S7. The particle size distribution of Co@NC-0 (a), Co@NC-0.3 (b), Co@NC-2 (c) and Co@NC-4 (d). It was founded that the mean sizes of different controlled samples were not changed too much.

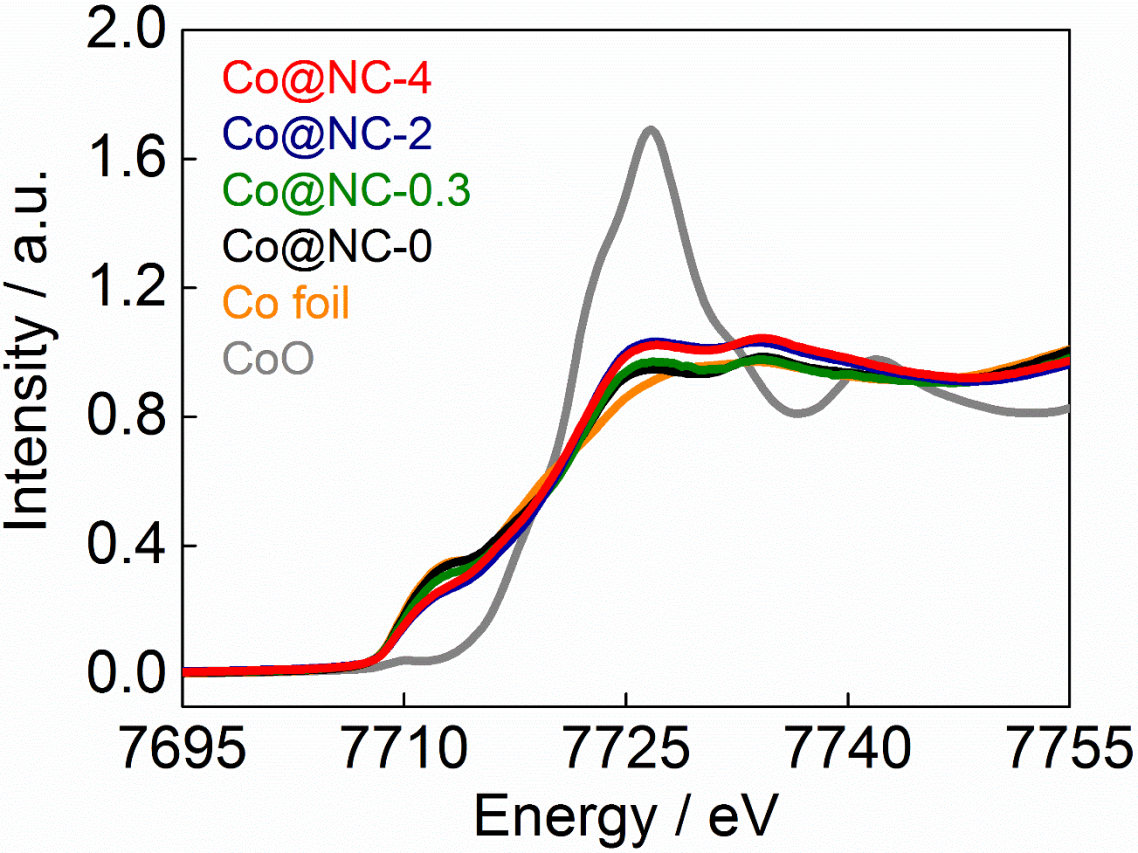

Figure S8. The normalized XANES spectra at the Co K-edge for Co@NC-x and referenced samples. The absorption threshold and edge of Co@NC-x didn't change obviously as compared with Co foil, suggesting the well-preserved metallic feature of Co components in Co@NC-x with different nitrogen contents.

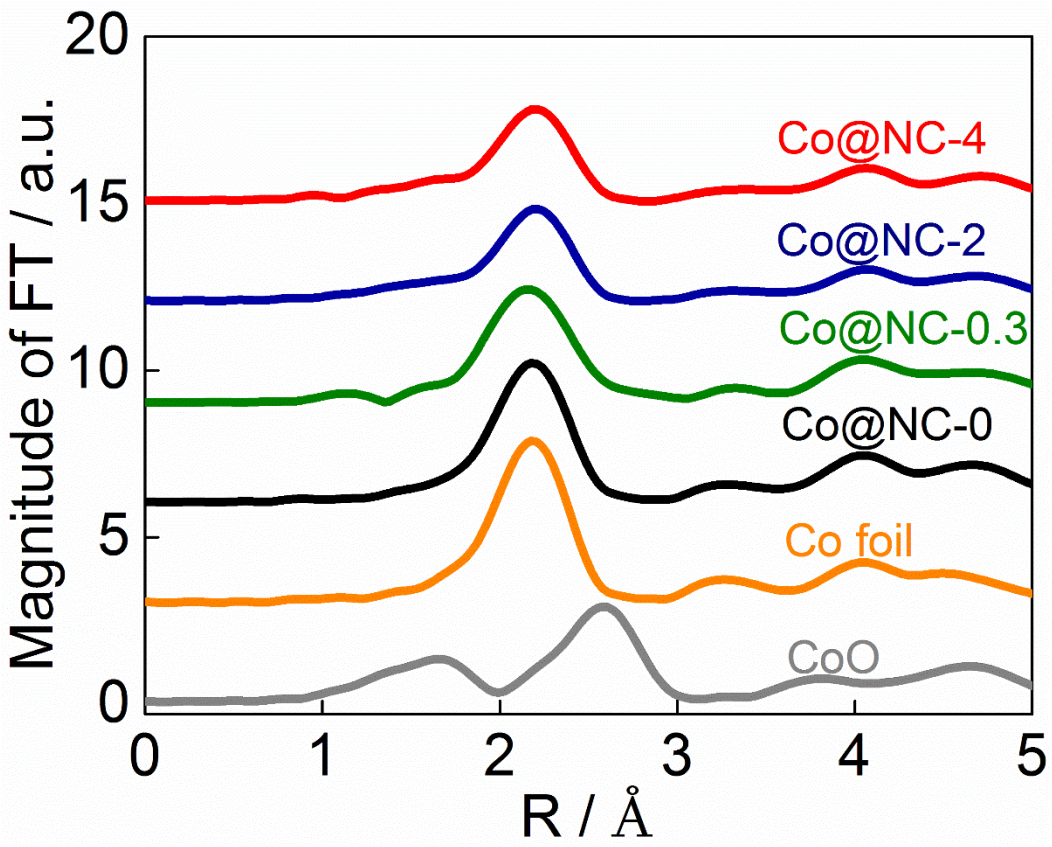

Figure S9. Fourier-transformed EXAFS spectra of Co@NC-x and referenced samples. Typical peaks of Co-X (X=N, C) at 1.41 Å and 2.76 Å were not observed in Co@NC-x samples. [S1-2] The amount of Co-O bonds is also negligible in our samples.

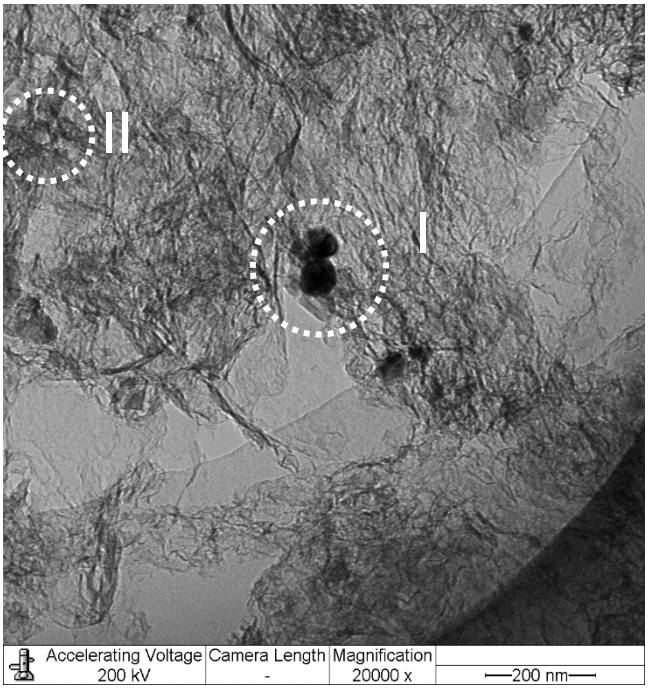

Figure S10. Typical TEM image of Co@NC-H^+. After acid etching, the Co nanoparticles encapsulated in thick carbon shell (I) and residual nitrogen-rich carbon hollow shell (II) were clearly presented.

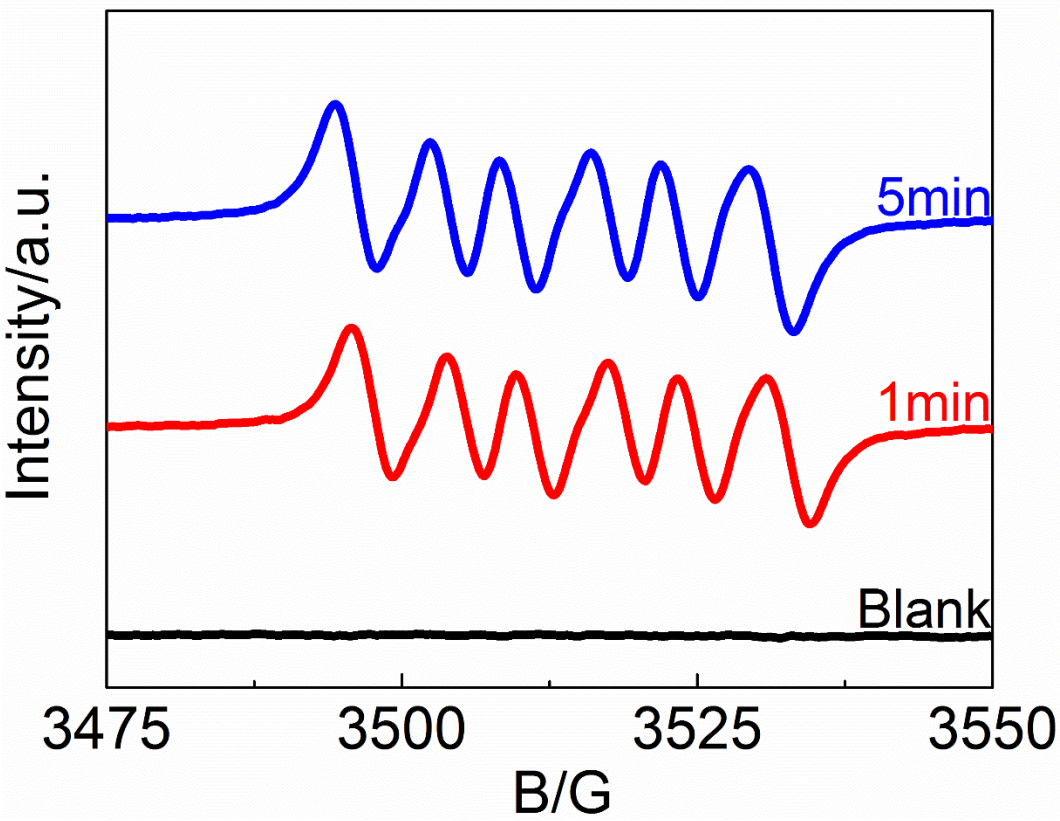

Figure S11. The DMPO (5,5-dimethyl-1-pyrroline *N*-oxide) spin-trapping EPR spectra for superoxide ($\bullet O_2^-$) in methanol (1 ml) in the presence of Co@NC-4 (2.5 mg) and benzyl alcohol (0.125 mmol). The typical signal of DMPO-$\bullet O_2H$ adducts directly demonstrated the formation of superoxide radical anion ($\bullet O_2^-$) in our catalytic system progresses. [S3] In our case, the oxidative deprotonation of H-metal intermediates results in the formation of $\bullet O_2H$.

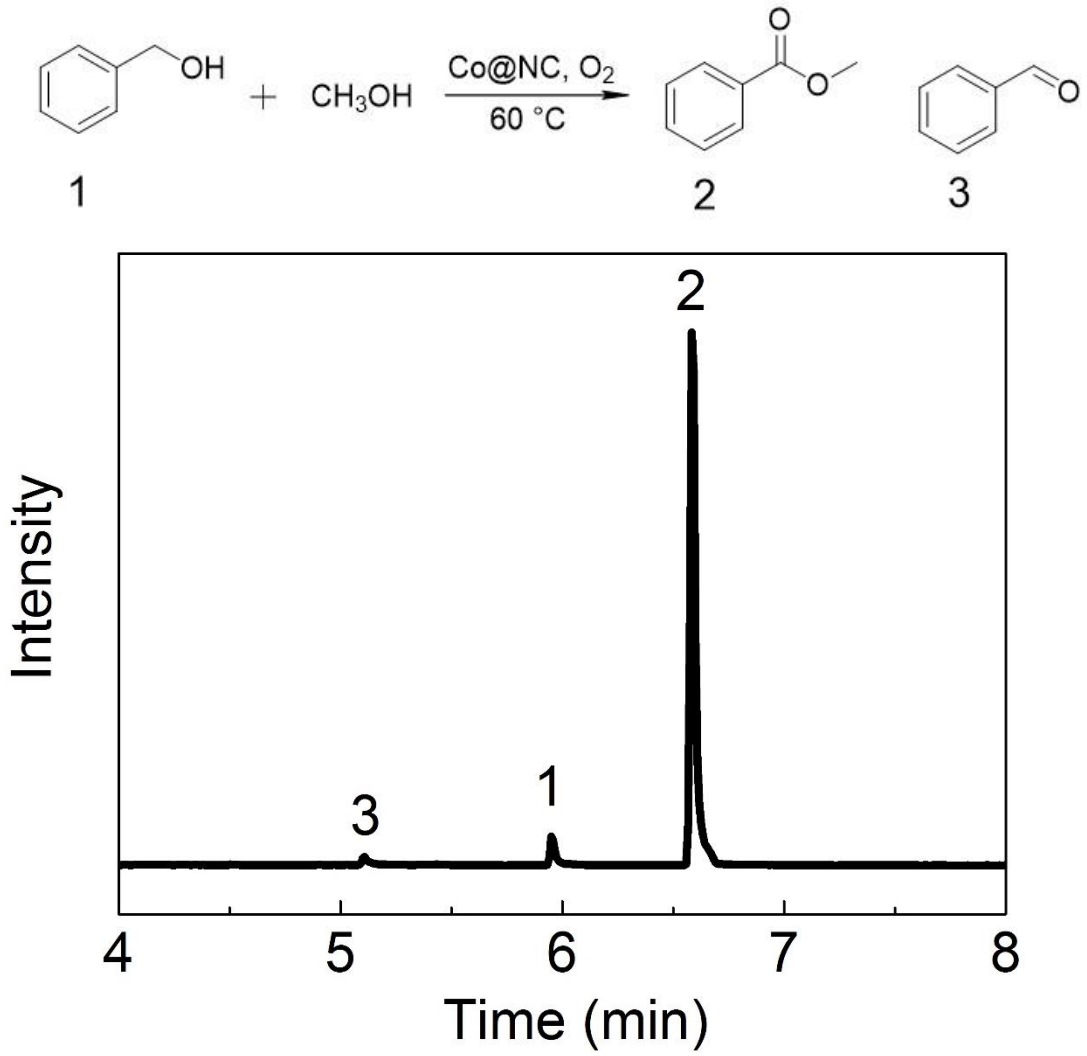

Figure S12. GC-MS spectra of the products from the aerobic esterification reaction of benzyl alcohol and methanol. Benzyl acid was not detected here.

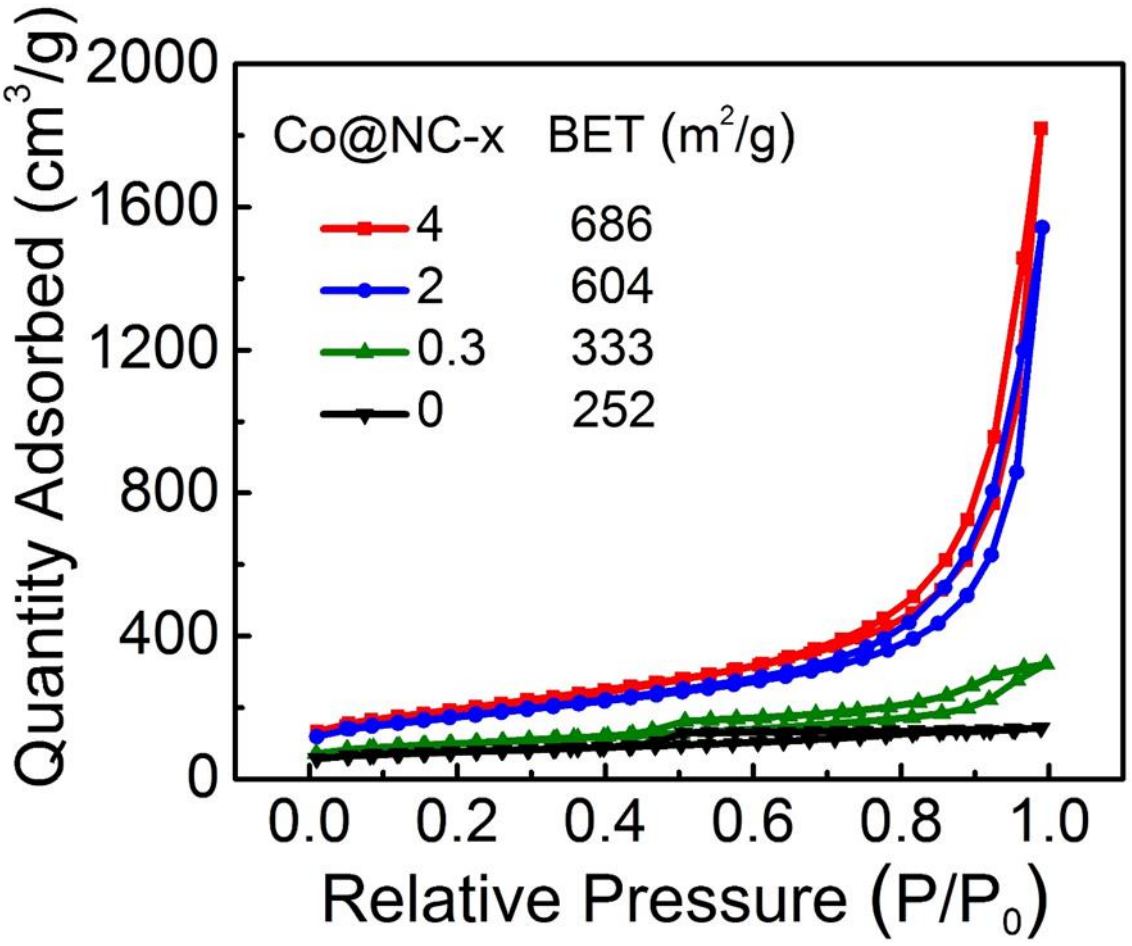

Figure S13. N_2 sorption isotherm curves of Co@NC-x. All samples afford moderate surface areas to ensure the reactants access to the Co nanoparticles. In the carbonization, difference of surface area in all samples is unavoidable after thermal decomposition of g-C_3N_4. The effect of surface area on the final catalytic activity was negligible here. The Co@NC-0 sample with a surface area to be only one third of that of Co@NC-4 was nearly inert for the base-free aerobic oxidation of alcohols. Moreover, the catalytic activity of Co@NC-4 was 2.8 times of that of Co@NC-2, eventhough their surface areas were not varied too much.

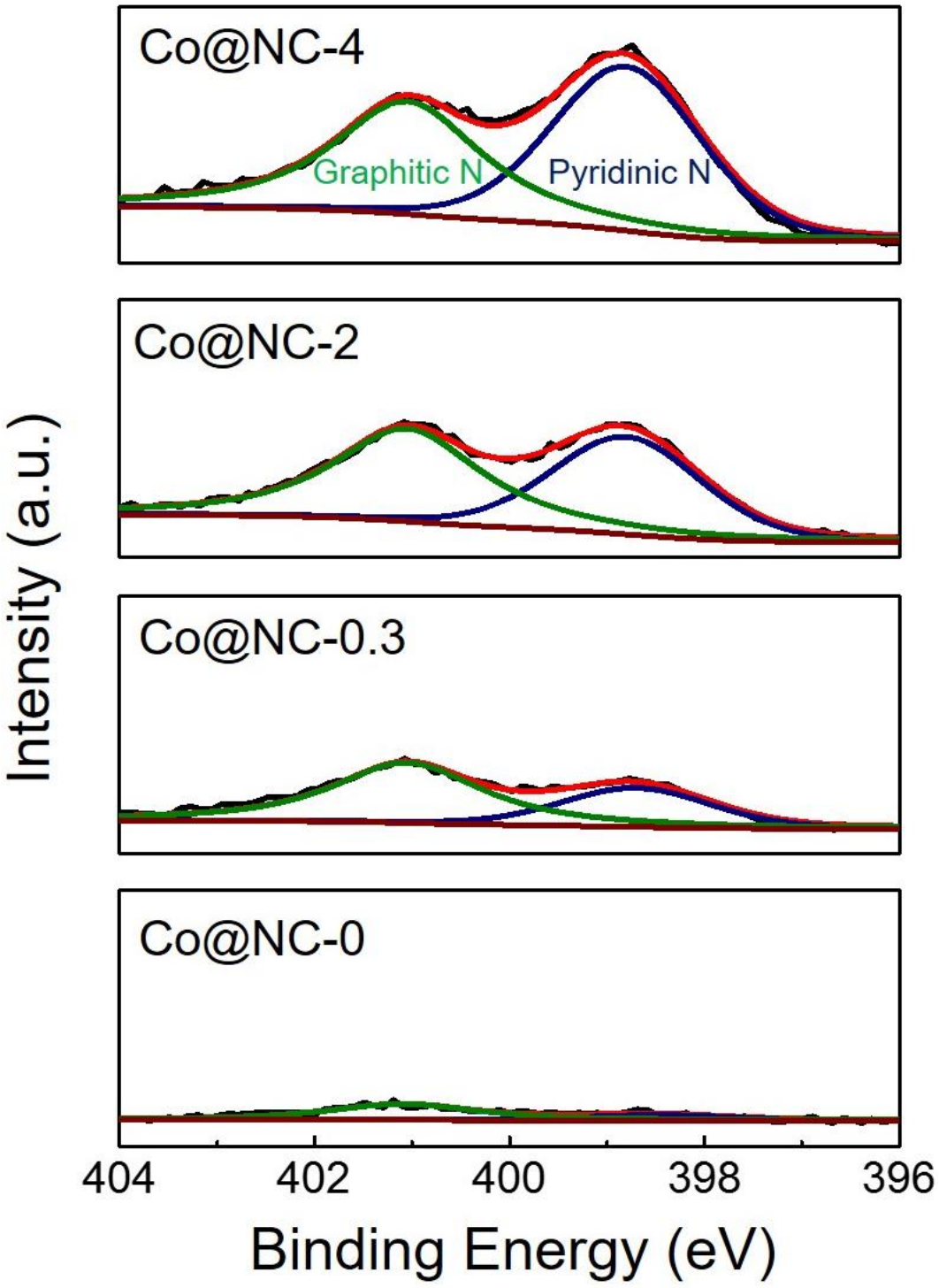

Figure S14. High resolution N 1s XPS spectra of Co@NC-x. Triethylene diamine molecules also act as nitrogen source for the formation of N-doped carbon in Co@NC-0, the doping level of which was rather lower and could not obviously activate the embedded Co nanoparticles (Figure 2a).

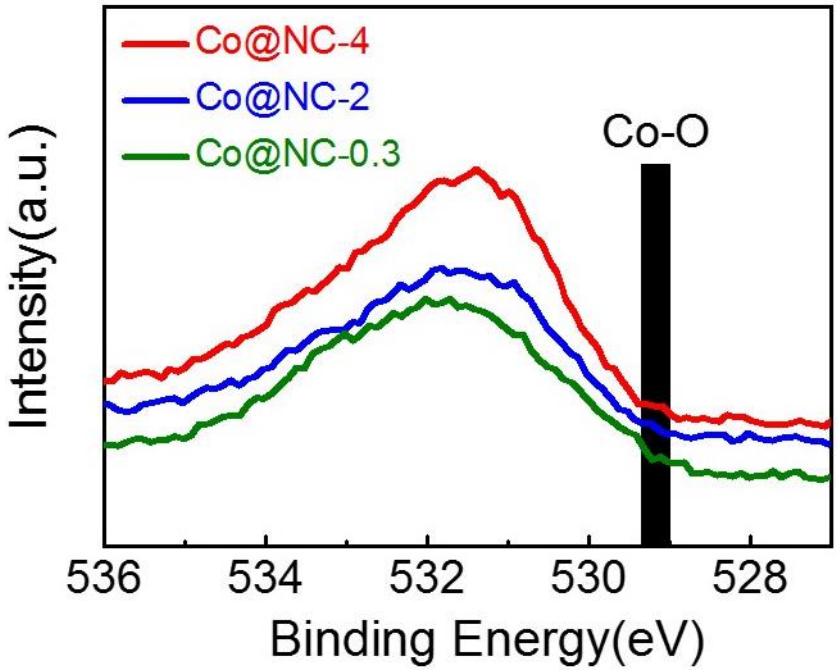

Figure S15. High resolution O 1s XPS spectra of Co@NC-x.

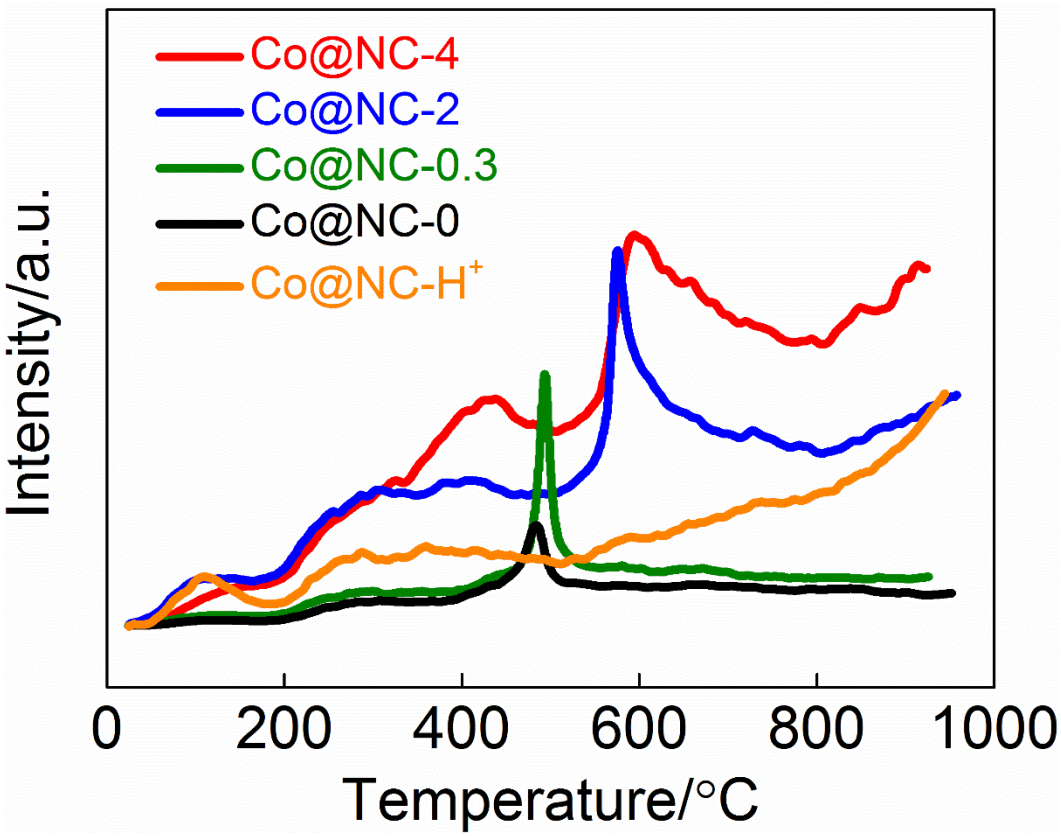

Figure S16. CO_2-TPD results of typical Co@NC-x samples. The CO_2 desorption peaks at low temperature were found in all nitrogen-rich samples. The weak functionality of bases is thus provided by the heteroatom N in carbon even in the Co@NC-H^+ sample, obtained after the removal of Co nanoparticles from Co@NC-4 via mild acid etching. A strong basic peak at around 500 ^oC in all Co-containing samples shifts to even higher temperature and also becomes even higher along with more nitrogen-dopants introduced into the carbon supports. Such a strong peak disappeared in Co@NC-H^+. All these results indicated that the strong basicity of the Co@NC-x dyads is induced by the interaction between Co nanoparticles and nitrogen-rich carbon supports, and could be tuned simply by introducing more nitrogen dopants to enhanced the interfacial interaction, that is the Mott-Schottky effect in solid state physics.

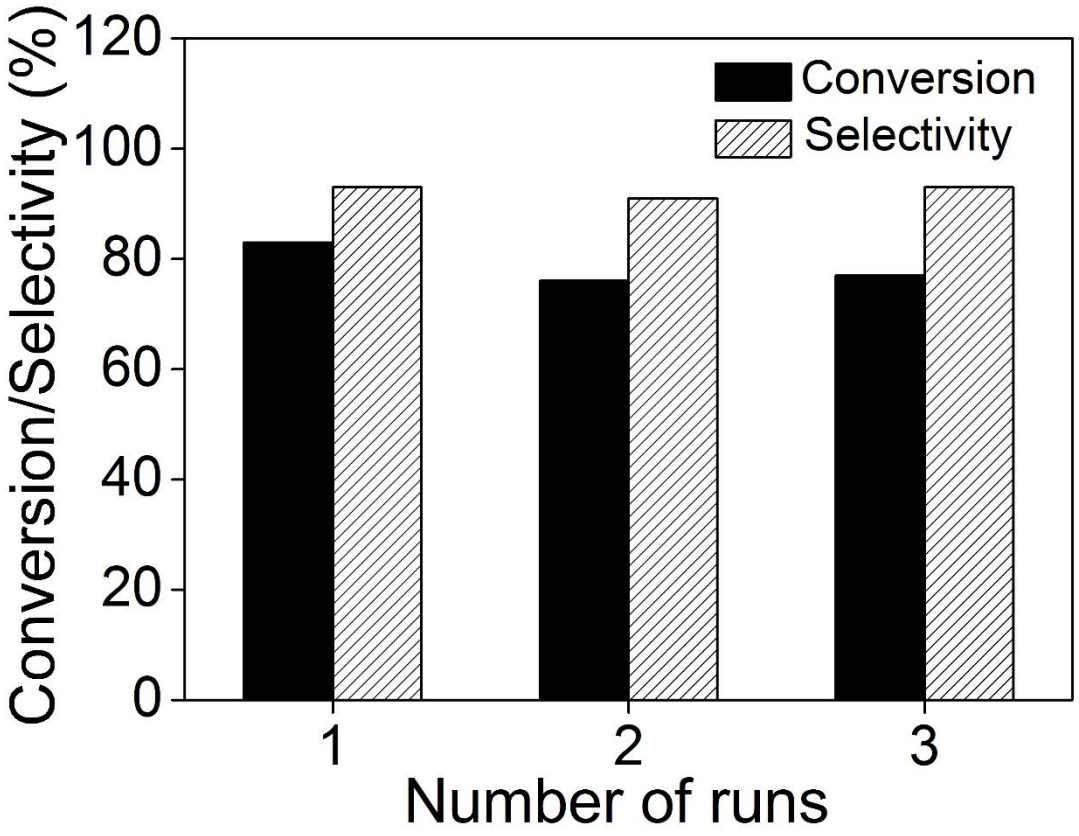

Figure S17. The conversion of benzyl alcohol and selectivity to methyl benzoate for aerobic esterification of benzyl alcohol over reused Co@NC-4 after washing by 0.1M NaOH. Reaction condition: 0.5 mmol benzyl alcohol, 4 mL of CH_3OH, Co@NC-4 (40mg), 60 °C, 3 h and 1 bar O_2. The catalyst was reused for 3 cycles by washing with 0.1M NaOH to remove protons and then pure methanol to remove all possible residues. The conversion and selectivity were determined by GC.

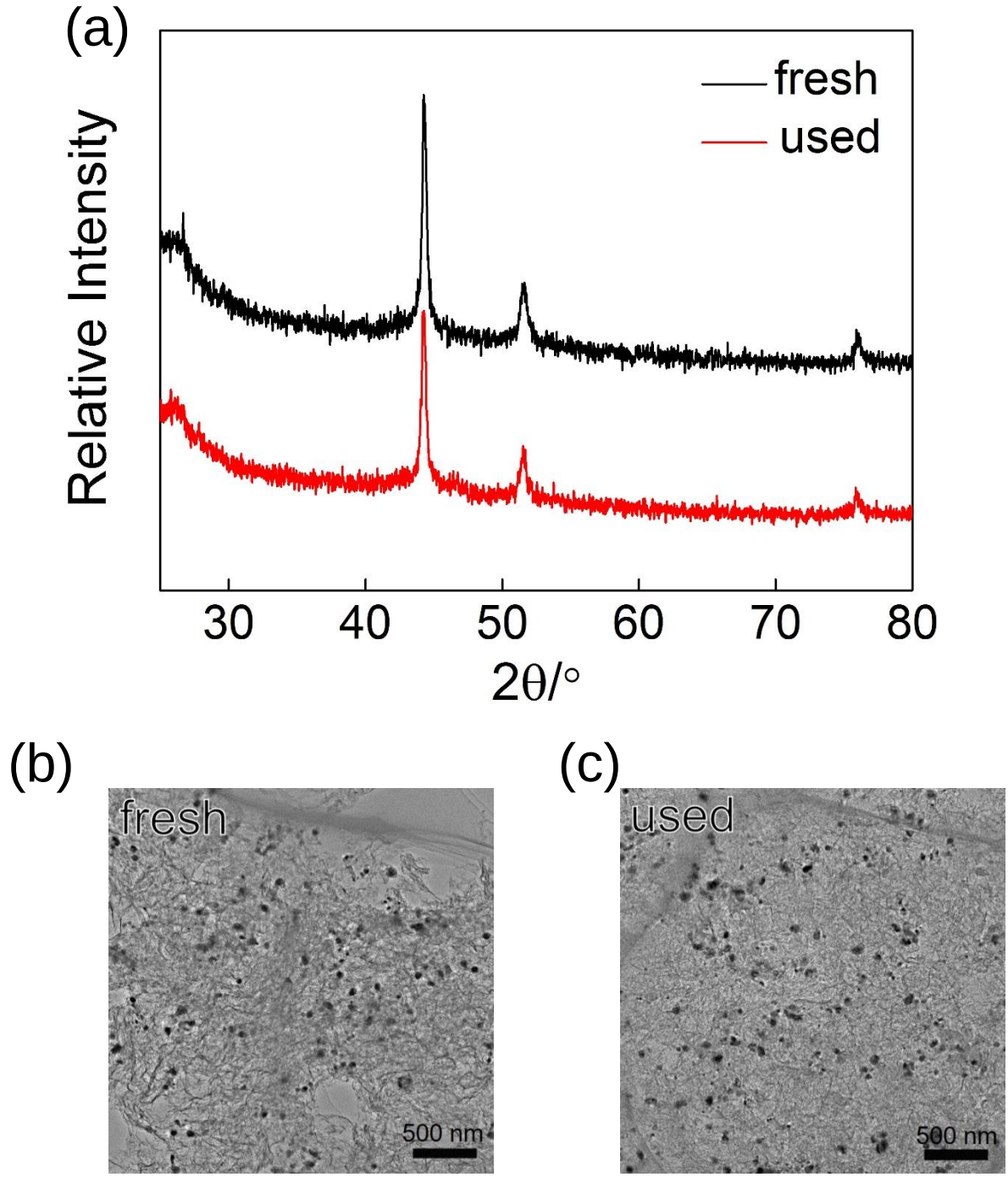

Figure S18. XRD patterns (a) and TEM images (b-c) of the fresh and used Co@NC-4 catalyst. All these observations well demonstrated the high stability of the nanocatalyst here.

Table S1. Elemental analysis results of Co@NC-x samples.

Sample	N (wt. %)	C (wt. %)	N/C (mol ratio %)
Co@NC-0	0.98	76.85	1.09
Co@NC-0.3	2.16	73.05	2.53
Co@NC-2	5.97	67.39	7.59
Co@NC-4	8.72	62.83	11.90
Co@NC-6	7.80	64.41	10.38

Table S2. Study results of reaction conditions

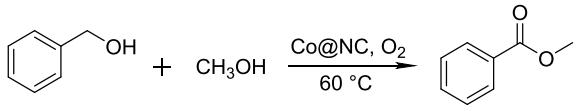

Entry	*Catalyst*	*t (h)*	*Con. (%)*	*Sel. (%)*
1	No catalyst	1	--	--
2	Co@NC-4 (N_2)	1	--	--
3	Co@NC-0	1	3	12
4	Co@NC-0.3	1	12	26
5	Co@NC-2	1	31	52
6	Co@NC-4	1	58	77
7	Co@NC-6	1	58	75
8	Co@NC-4	4	77	88
9	Co@NC-4	8	88	93
10	Co@NC-4	12	99	98
11	Co@NC-4-H^+	12	trace	--
12[b]	Co@NC-4	12	30	21
13[c]	Co@NC-4	12	40	96
14[d]	Co@NC-4	12	31	35

[a] standard condition: 0.5 mmol benzyl alcohol, 4 mL of CH_3OH, 5.5 mol % Co catalyst, 60 °C and 1 bar O_2. [b] 0.2 mmol KSCN was added. [c] 0.5 mmol benzaldehyde served as substrate. [d] The terminal agent 0.2 mmol butylated hydroxytoluene (BHT) was added. The by-product was benzaldehyde for all entries.

Table S3. Results of direct benzyl alcohol esterification with base.

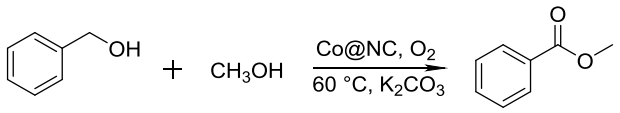

Entry	*Catalyst*	*Time (h)*	*Con. (%)*	*Sel. (%)*
1	Co@NC-0	1	7	18
2	Co@NC-0.3	1	21	69
3	Co@NC-2	1	70	92
4	Co@NC-4	1	89	98
5	Co@NC-6	1	86	96

Catalysis condition: 0.5 mmol benzyl alcohol, 0.1 mmol K_2CO_3, 4 mL of CH_3OH, 5.5 mol % Co catalyst, 60 °C and 1 bar O_2. The conversion and selectivity were determined by GC. The by-product was benzaldehyde for all entries.

Table S4. The TON of selected entries Table S2 in terms of the total amount of benzyl alcohol converted per mole of metal catalyst

Entry	6	8	9	10
Con. (%)	58	77	88	99
TON	10.5	14	16	18

Table S5. Summary of results reported for aerobic esterification of benzyl alcohol under base-free condition.

Catalyst	Condition	TOF(h^{-1})	Reference
Co@NC	1bar O_2, base-free, 60°C, 1h	8.12	This work
Co_3O_4-N@C	1bar O_2, base-free, 60°C, 24h	0.25	J. Am. Chem. Soc. **2013**, 135, 10776
Co-CoO@NC	1bar O_2, base-free, 80°C, 12h	0.036	Chem. Commun. **2015**, 51, 8292
Co@C-N	1bar air, base-free, 25°C, 96h	0.069	ACS Catal. **2015**, 5, 1850

Reaction parameters in this work were adapted from Reference (J. Am. Chem. Soc. **2013**, 135, 10776).

The TOF value was calculated in the format of mol MB mol^{-1} metal h^{-1}. The amount of metal is based on the moles of metal components involved.

Table S6. Summary of results reported for aerobic esterification of benzyl alcohol with base.

Catalyst	Condition	TOF(h^{-1})	Reference
Co@NC-4	1bar O_2, 0.2 Equiv. K_2CO_3, 60°C, 1h	15.86	This work
Co_3O_4-N@C	1bar O_2, 0.2 Equiv. K_2CO_3, 60°C, 24h	1.62	J. Am. Chem. Soc. **2013**, 135, 10776
Co_3O_4/Al_2O_3	1bar O_2, 0.2 Equiv. K_2CO_3, 60°C, 24h	1.32	J. Am. Chem. Soc. **2013**, 135, 10776
Co_3O_4/TiO_2	1bar O_2, 0.2 Equiv. K_2CO_3, 60°C, 24h	0.75	J. Am. Chem. Soc. **2013**, 135, 10776
Co-CoO@NC	1bar O_2, 0.2 Equiv. K_2CO_3, 80°C, 12h	0.60	Chem. Commun. **2015**, 51, 8292

Reaction parameters in this work were adapted from Reference (J. Am. Chem. Soc. **2013**, 135, 10776).

The TOF value was calculated in the format of mol MB mol^{-1} metal h^{-1}. The amount of metal is based on the moles of metal components involved.

Table S7. Results of aerobic esterification of ortho-sustituted benzyl alcohol.

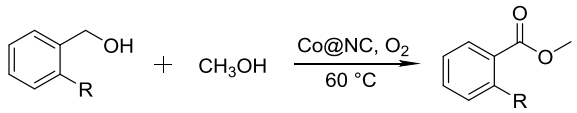

Entry	*substrate*	*Mass (mg)*	*Time(h)*	*Con. (%)*	*Sel. (%)*
1	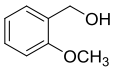	10mg	12	99	36
2	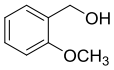	10mg	24	99	36
3	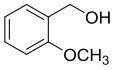	10mg	48	99	45
4	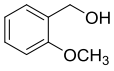	25mg	12	99	45
5	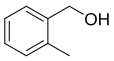	10mg	12	72	57
6	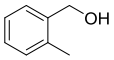	10mg	24	83	67
7	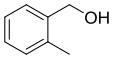	25mg	12	79	72

Catalysis condition: 0.5 mmol substrates, 4 mL of CH_3OH, 5.5 mol % Co catalyst, 60 °C and 1 bar O_2. The conversion and selectivity were determined by GC. The by-product was ortho-sustituted benzaldehyde for all entries.

Table S8. Optimizing the catalyst ratio for base-free cross-esterification of benzyl alcohol and ethanol under condition.

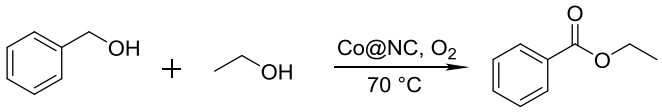

Entry	*Mass*	*Time(h)*	*Con. (%)*	*Sel. (%)*
1	10mg	12	72	53
2	25mg	12	93	72
3	25mg	24	93	72
4	40mg	12	99	88

Catalysis condition a: 0.1 mmol benzyl alcohol, 4 mL of ethanol, Co@NC-4, 70 °C and 1 bar O_2. The conversion and selectivity were determined by GC-MS. The by-product was benzaldehyde for all entries.

References

[S1] Yin, P. Q.; Yao, T.; Wu, Y.; Zheng, L, R.; Lin, Y.; Liu, W.; Ju, H. X.; Zhu, J, F.; Hong, X.; Deng, Z. X.; Zhou, G.; Wei, S. Q.; Li, Y. D. *Angew. Chem. Int. Ed.* **2016**, *55*, 10800-10805

[S2] Liu, W. G.; Zhang, L. L.; Yan, W. S.; Liu, X. Y.; Yang, X. F.; Miao, S.; Wang, W. T.; Wang, A. Q.; Zhang, T. *Chem. Sci.* **2016,** *7*, 5758-5764.

[S3] Yao, Y. Y.; Wang, L.; Sun, L. J.; Zhu, S.; Huang, Z. F.; Mao, Y. J.; Lu, W. Y.; Chen, W. X. *Chem. Eng. Sci.* **2013**, *101*, 424-431.